

New Dynamic Programming Algorithm for the Multiobjective Minimum Spanning Tree Problem

Pedro Maristany de las Casas Antonio Sedeño-Noda
Ralf Borndörfer

May 01, 2023

Abstract

The *Multiobjective Minimum Spanning Tree* (MO-MST) problem is a variant of the Minimum Spanning Tree problem, in which the costs associated with every edge of the input graph are vectors. In this paper, we design a new dynamic programming MO-MST algorithm. Dynamic programming for a MO-MST instance leads to the definition of an instance of the One-to-One Multiobjective Shortest Path (MOSP) problem and both instances have equivalent solution sets. The arising MOSP instance is defined on a so called transition graph. We study the original size of this graph in detail and reduce its size using cost dependent arc pruning criteria. To solve the MOSP instance on the reduced transition graph, we design the Implicit Graph Multiobjective Dijkstra Algorithm (IG-MDA), exploiting recent improvements on MOSP algorithms from the literature. All in all, the new IG-MDA outperforms the current state of the art on a big set of instances from the literature. Our code and results are publicly available.

1 Introduction

We consider the *Multiobjective Minimum Spanning Tree* (MO-MST) problem. An instance of the problem is a tuple (G, c, s) consisting of an undirected connected graph $G = (V, E)$, a d -dimensional edge cost functions $c : E \rightarrow \mathbb{R}_{\geq 0}^d$, and a node $s \in V$ that is assumed, w.l.o.g, to be the root of every spanning tree in G . Trees in G are connected acyclic subgraphs. Moreover, we characterize any tree t in G by its edges, i.e., $t \subseteq E$. Then, the costs of t are defined as $c(t) := \sum_{e \in t} c(e) \in \mathbb{R}_{\geq 0}^d$ and we refer to the set of nodes spanned by t by $V(t) \subseteq V$. We use the notions *efficiency* and *non-dominance* to refer to *optimal* trees.

Definition 1. Consider a MO-MST instance (G, c, s) . Let t, t' be trees in G . t *dominates* t' if $V(t) = V(t')$, $c(t) \leq c(t')$, and $c(t) \neq c(t')$. Moreover, t is an *efficient* tree, if it is not dominated by any other tree. The cost vector of an efficient spanning tree of V is called an *nondominated cost vector*.

In this paper we are interested in computing *minimum complete sets of efficient trees*: a subset of the efficient spanning trees of a given graph G w.r.t. an edge cost function c s.t. for every nondominated cost vector, there is exactly one efficient tree in the subset. We use the $*$ -operator to denote minimum complete sets of a given set of edges or trees.

Definition 2. For a discrete set $Y \subset \mathbb{R}_{\geq 0}^d$, $Y^* \subseteq Y$ is the unique set of nondominated vectors in Y . Consider an undirected graph $G = (V, E)$ and a d -dimensional edge cost function c . Let X be a set of edges or trees in G and define $c(X) := \{c(x) \mid x \in X\} \subset \mathbb{R}_{\geq 0}^d$. Then, $c(X)^*$ is well defined and we define $X^* \subseteq X$ to be a subset of X with minimum cardinality s.t. $c(X^*) = c(X)^*$.

Formally we can now define the MO-MST as follows.

Definition 3 (Multiobjective Minimum Spanning Tree Problem). Consider an undirected graph $G = (V, E)$, a root node $s \in V$, and d -dimensional edge cost functions $c : E \rightarrow \mathbb{R}_{\geq 0}^d$. Let T be the set of all spanning trees of G . The *Multiobjective Minimum Spanning Tree* (MO-MST) problem is to find a minimum complete set $T^* \subseteq T$ of efficient trees according to Definition 2. We refer to the pair (G, c, s) as a *d -dimensional MO-MST instance*.

On a complete graph with $n \in \mathbb{N}$ labeled nodes there are n^{n-2} spanning trees [Cayley, 2009]. Hamacher and Ruhe [1994] constructed bidimensional MO-MST instances on complete graphs in which every spanning tree has a nondominated cost vector, proving the problem’s intractability. In their paper, they also include a result that proves the NP-hardness of the MO-MST problem.

1.1 Literature Review and Outline

The MO-MST problem is well studied in the literature. For good introduction to the topic with multiple insights on different solution approaches, we refer to [Ehrgott, 2005, Section 9.2.]. The recent survey by Fernandes et al. [2020] benchmarks different algorithms on a huge set of instances providing good insights on what techniques work best in practice nowadays.

For the classical Minimum Spanning Tree problem, greedy approaches like the well known algorithms by Kruskal [1956] or by Prim [1957] are very efficient in theory and in practice. However, extrapolating these techniques to a multiobjective scenario like ours does not deliver good algorithmic performance. A good explanation is given in [Ehrgott, 2005, Section 9.2]. In a nutshell, the main reason is that with higher dimensional edge costs, cost-minimal edge to be included in every iteration are not well defined.

This observation opens up the search for new algorithmic approaches to solve minimum spanning tree problems in multiobjective scenarios. Interestingly, this search leads to different answers depending on the problem’s dimension. In the biobjective case two phase algorithms [Hamacher and Ruhe, 1994, Ramos et al., 1998, Steiner and Radzik, 2008, Sourd and Spanjaard, 2008, Amorosi and Puerto, 2022] have been proven to be most efficient. These algorithms compute the supported efficient spanning trees in the first phase and the unsupported efficient solutions in the second. Supported solutions are obtained solving multiple instances of the single criteria Minimum Spanning Tree problem via scalarization of the objective functions. For the computation of unsupported solutions, different techniques are used. In their state of the art algorithm Sourd and Spanjaard [2008] split the second phase into two subphases. First they find unsupported solutions performing neighborhood search starting from the already found efficient trees. Finally the missing efficient trees are found solving multiple MIPs that use the costs of the existing efficient trees as bounds. The reason for the superb performance of this algorithm is that in almost every practical instance, all efficient trees are already computed after the neighborhood search.

For edge costs with more than two dimensions, efficient two phase approaches are not known as discussed for example in [Ehrgott and Gandibleux, 2000]. This once again opens up the search for efficient algorithms leading to dynamic programming algorithms. In this context, two publications by Di Puglia Pugliese, Guerreiro, and Santos stand out. They first published a dynamic programming algorithm for the MO-MST problem in [Di Puglia Pugliese et al., 2014] and afterwards they notably improved their approach in [Santos et al., 2018] designing the *BN algorithm*. In it they include an elegant way of ensuring that every dynamically built tree is only considered once. By doing so, they solve an arising *symmetry* issue in their original algorithm.

Outline We start Section 2 embedding the MO-MST problem in a dynamic programming context. Then, similar to [Santos et al., 2018, Section

3.1, Section 3.2], we discuss how to transform a MO-MST instance into an instance of the One-to-One Multiobjective Shortest Path (MOSP) problem defined on a so called transition graph \mathcal{G} . Both instances' solution sets are equivalent. In Section 2.1 to Section 2.4 we discuss our first main contributions: how to reduce the size of \mathcal{G} . The resulting One-to-One MOSP instance defined on the reduced transition graph is used in our second main contribution: the Implicit Graph Multiobjective Dijkstra Algorithm (IG-MDA) introduced in Section 3. It features multiple recent techniques to efficiently solve large scale MOSP instances [Pulido et al., 2014, Sedeño-Noda and Colebrook, 2019, Maristany de las Casas et al., 2021b,a]. We also use these techniques in our implementation of the BN algorithm. It is described in A. In Section 4 we present the results of our computational experiments in which we benchmark the IG-MDA against the BN algorithm. Since on bidimensional MO-MST instances both algorithms are clearly outperformed by the two phase algorithm from Sourd and Spanjaard [2008], we use three and four dimensional instances in our experiments. We consider all such MO-MST instances from [Santos et al., 2018] and a big subset of the instances used in [Fernandes et al., 2020]. Thereby, we achieve the last contribution in this paper: to the best of our knowledge the size of the solved instances is bigger than so far in the literature.

2 Dynamic Programming for MO-MST

In dynamic programming, bellman conditions are recursive expressions that state how to derive efficient solutions for a problem at hand from efficient solutions of its subproblems. In our MO-MST scenario, the Bellman condition (cf. Theorem 5) states how to build efficient spanning subtrees of a subset $W \subseteq V$ by looking at the efficient spanning subtrees of all subsets $U \subset W$ with $|U| = |W| - 1$.

Recall that any node set $U \subseteq V$ induces the *cut*

$$\delta(U) := \{[u, w] \in E \mid u \in U, w \in V \setminus U\}$$

and we have the following basic result from graph theory.

Lemma 4. *Let $G = (V, E)$ be an undirected graph, t a tree in G , and $[u, w] \in E$ an edge. Then, $t' = t \circ [u, w]$ is a tree if and only if $[u, w] \in \delta(V(t))$. If that is the case, we have $|V(t)| = |V(t')| - 1$.*

We refer to the subgraph induced by a node set $U \subseteq V$ by $G(U)$. Additionally, the spanning trees of $G(U)$ are denoted by $T_{G(U)}$. Recall that the $*$ -operator is defined in Definition 2.

Theorem 5 (Bellman Condition for Efficient Subtrees). *Let $(G = (V, E), c, s)$ be a d -dimensional MO-MST instance.*

Base Case *We set $t_{G(\{s\})}$ to be the spanning tree of $G(\{s\})$, a subgraph containing just the node s and no edges, and $c(t_{G(\{s\})}) = 0$. Since this is the only tree in $T_{G(\{s\})}$, we have $T_{G(\{s\})} = T_{G(\{s\})}^*$.*

Recursion *Consider a subset $W \subseteq V$ of cardinality $k \in \{2, \dots, n\}$. A minimum complete set of efficient spanning trees of $G(W)$ is given by*

$$T_{G(W)}^* = \left\{ t' \circ [u, w] \mid t' \in T_{G(U)}^*, U \subset W, |W| = |U| + 1, \text{ and } [u, w] \in \delta(U) \right\}^*. \quad (1)$$

Proof. Assume there exists an efficient spanning tree t of W and a subset $U \subset W$ s.t. $t = t'' \circ [u, w]$ for a dominated tree t'' of U . Consider an efficient spanning tree t' of U that dominates t'' . $t' \circ [u, w]$ is also a spanning tree of W (Lemma 4) and

$$c(t') \leq c(t'') \Leftrightarrow c(t' \circ [u, w]) \leq c(t'' \circ [u, w]) = c(t).$$

Since t' dominates t'' the first inequality is strict for at least one index causing t to also be dominated. By Lemma 4 every spanning tree of W can be obtained from spanning trees of $U \subset W$ with $|U| + 1 = |W|$. Then, the correctness of the statement follows by induction over the cardinality of $|W|$ and using $T_{G(\{s\})} = T_{G(\{s\})}^*$ as the induction's base case.

Note that the $*$ -operator on the right hand side of (1) is needed because the expansions of efficient trees of different subsets U of W can dominate each other. \square

In the remainder of this section, we discuss how to exploit the efficiency condition derived in Theorem 5. For a given MO-MST instance $(G = (V, E), c)$ we define a so called *transition graph* $\mathcal{G} = (\mathcal{V}, \mathcal{A})$ where each *transition node* in \mathcal{V} represents a subset of nodes in G . Our goal is to define \mathcal{G} in such a way that efficient paths from the transition node $\{s\}$ to the transition node that represents the whole node set V correspond to efficient spanning trees of G .

Definition 6 (One-to-One Multiobjective Shortest Path Problem). Given a directed graph $\mathcal{V} = (\mathcal{V}, \mathcal{A})$, a cost function $\gamma : \mathcal{A} \rightarrow \mathbb{R}_{\geq 0}^d$, a source node $\{s\} \in \mathcal{V}$, and a target node $V \in \mathcal{V}$, the One-to-One Multiobjective Shortest Path problem is to find a minimum complete set of efficient $\{s\}$ - V -paths in \mathcal{G} w.r.t. γ . We refer to the tuple $(\mathcal{G}, \gamma, \{s\}, V)$ as a problem's instance.

Our exposition from Definition 7 to Theorem 10 is similar to [Santos et al., 2018, Section 3.1]. Note that for a discrete set X , the power set of X is 2^X . In the definition of \mathcal{G} we incur in a slight abuse of notation when denote a transition node U and simultaneously mean the transition node in \mathcal{V} and the subset $U \subseteq V$ of nodes in the original graph G .

Definition 7 (Transition Graph). Consider a MO-MST instance $(G = (V, E), c, s)$. We define the *transition graph of G* as the directed graph $\mathcal{G} = (\mathcal{V}, \mathcal{A})$ with node set $\mathcal{V} := \{V' \cup \{s\} \mid V' \in 2^{V \setminus \{s\}}\}$. Every such node is also called a *transition node*. The outgoing arcs of node $U \in \mathcal{V}$ are induced by the cut $\delta(U)$:

$$\delta^+(U) := \left\{ (U, W) \mid W = U \cup \{w\} \text{ if } \exists [u, w] \in \delta(U) \right\}. \quad (2)$$

The set of arcs in \mathcal{G} is given by $\mathcal{A} := \bigcup_{U \in \mathcal{V}} \delta^+(U)$. For an arc $(U, W) \in \mathcal{A}$ we denote the unique *preimage edge* $[u, w] \in E$ that induces it by $(U, W)^{-1}$ and we refer to (U, W) as a *copy of $[u, w]$ in \mathcal{G}* . We define a d -dimensional arc cost function $\gamma : \mathcal{A} \rightarrow \mathbb{R}_{\geq 0}^d$ setting $\gamma(a) = c(a^{-1})$.

Note that for an arc (U, W) as defined in (2), we have $U, W \in \mathcal{V}$ and $U \cup \{w\} = W$ for some node $w \in V$, i.e., W is an expansion of U by just one node. Even though we defined the set \mathcal{A} using the nodes' outgoing arcs, it of course also allows us to access sets $\delta^-(U)$ of incoming arcs for every transition node U . The following remark is important for the understanding of the remainder of this section.

Remark 1. The transition graph $\mathcal{G} = (\mathcal{V}, \mathcal{A})$ as defined in Definition 7 is a layered acyclic multigraph.

Layered For $k \in \{1, \dots, n\}$ the k^{th} layer of \mathcal{G} consists of all nodes in \mathcal{V} that encode a subset of nodes in V with cardinality k .

Acyclic From (2) we immediately see that \mathcal{A} only contains arcs connecting neighboring layers and that the arcs always point towards the layer of greater cardinality.

Multigraph \mathcal{A} is a multiset: multiple arcs connect the same pairs of nodes in \mathcal{G} . Parallel arcs might have different costs depending on their preimage edge. Additionally, for two parallel arcs $a, b \in \mathcal{A}$, there always holds $a^{-1} \neq b^{-1}$.

Figure 1 includes an example of a MO-MST instance and its corresponding One-to-One MOSP instance.

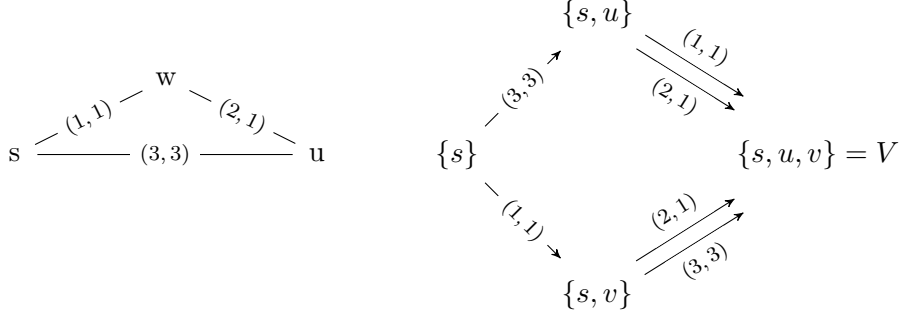


Figure 1: Left: 2d MO-MST instance (G, c, s) . Right: Corresponding One-to-One MOSP instance $(\mathcal{G}, \gamma, \{s\}, V)$

The following definition formalizes the intuition of a path in \mathcal{G} representing a tree in G .

Definition 8 (Path Representations of a tree). Consider a MO-MST instance (G, c, s) and the associated transition graph \mathcal{G} . For a node $U \in \mathcal{V}$ an $\{s\}$ - U -path p in \mathcal{G} is said to *represent* or *be a representation* of a spanning tree t of U in G if $t = \{a^{-1} \mid a \in p\}$.

The following lemma describes the mapping between trees in G and paths in \mathcal{G} and their cost equivalence. Thereby it is important to note that a tree is represented by multiple paths but a path represents only one tree. The omitted proof corresponds to the proofs in [Santos et al., 2018, Proposition 3.1., Proposition 3.2.].

Lemma 9. *A tree t in G rooted at s and spanning a node subset $U \subseteq V$ is represented in \mathcal{G} by at least one $\{s\}$ - U -path. For any such path p we have $c(t) = \gamma(p)$. Conversely, an $\{s\}$ - U -path in \mathcal{G} for some $U \in \mathcal{V}$ represents a tree t in G and $\gamma(p) = c(t)$.*

We can now conclude that a given MO-MST instance can be solved computing the efficient paths in a One-to-One MOSP instance on the induced transition graph.

Theorem 10. *Consider a subset $U \subseteq V$ that contains s . A minimum complete set of efficient $\{s\}$ - U -paths in \mathcal{G} w.r.t. γ corresponds to a minimum complete set of efficient spanning trees of U in G w.r.t. c .*

Proof. Let P_U the set of $\{s\}$ - U -paths in \mathcal{G} . By Lemma 9 every such path represents a spanning tree of U in G and all spanning trees of U are represented by at least one of these paths. Moreover, we have $\gamma(P_U) = c(T_{G(U)})$ and as a consequence, $\gamma(P_U)^* = c(T_{G(U)})^*$ which finishes the proof. \square

2.1 Size of the transition graph

In this section, we consider a d -dimensional MO-MST instance $(G = (V, E), c)$ in which G is a complete graph with n nodes. Additionally, we again assume that all spanning trees are rooted at a node $s \in V$ and build the equivalent One-to-One MOSP instance $(\mathcal{G}, \gamma, \{s\}, V)$ as defined in Definition 7.

For a subset $U \subseteq V$ that contains s , let t be a spanning tree of $G(U)$ with depth one. Then, there are $(|U| - 1)!$ $\{s\}$ - U -paths in \mathcal{G} . This number of representations of a tree in \mathcal{G} is an upper bound because for trees with depth greater than one, the ordering of the edges along the root-to-leaf paths in the tree have to be respected along the $\{s\}$ - U -paths in \mathcal{G} . If the spanning tree t is a path, then the representation of t in \mathcal{G} by a $\{s\}$ - U -path is unique.

In our setting, having fixed a node as the root node of all spanning trees, it is easy to see that for any $k \in \{1, \dots, n\}$ the k^{th} layer (cf. Remark 1) of nodes in \mathcal{V} is build out of $\binom{n-1}{k-1}$ nodes. Thus, we obtain

$$|\mathcal{V}| = \sum_{k=1}^n \binom{n-1}{k-1} = 2^{n-1}. \quad (3)$$

The overall number of arcs between layer k and layer $k + 1$ for any $k \in \{1, \dots, n\}$ is

$$\binom{n-1}{k-1} (n-k)k \quad (4)$$

where the first multiplier is the number of transition nodes in the k^{th} layer, the second multiplier is the number of missing nodes from G in any subset of nodes of G with cardinality k , and the last multiplier accounts for the number of parallel arcs. Thus, all in all, the number of arcs in \mathcal{G} is

$$|\mathcal{A}| = \sum_{k=1}^n \binom{n-1}{k-1} (n-k)k = 2^{n-3} (n-1)n \quad (5)$$

Clearly, the size of the transition graph \mathcal{G} is an issue to address in the development of efficient dynamic programming algorithms for MO-MST problems. In the following sections, we discuss different techniques to reduce the size of \mathcal{G} . In Section 2.2, we discuss a polynomial running time approach

that acts on the input graph G directly recognizing edges that can be deleted from the graph or edges that can be included in every efficient spanning tree. In Section 2.3 and Section 2.4, we discuss criteria to reduce the size of \mathcal{A} . These criteria are cut-dependent and are applied during the construction of the sets $\delta^+(U)$ for $U \in \mathcal{V}$.

2.2 Polynomial time graph reduction during preprocessing

The manipulation of the input graph G described in this section is explained in [Sourd and Spanjaard, 2008]. We refer the reader to the original paper to understand the details and correctness proofs. An edge $e \in E$ can be irrelevant for the MO-MST search, if e is not contained in any efficient spanning tree of G or if for every non dominated cost vector, there exists a spanning tree with this cost that contains e .

Definition 11 (Red and Blue Arcs. cf. [Sourd and Spanjaard, 2008], Section 3.2). Consider an instance (G, c, s) of the MO-MST problem and let T_G be the set of spanning trees of G w.r.t. c .

Blue edge An edge $e \in E$ is *blue* if for every non-dominated cost vector in $c(T_G)^*$ there is an efficient tree $t \in T_G$ that contains e .

Red edge An edge $e \in E$ is *red* if it is not contained in any tree contained in a minimum complete set T_G^* of efficient spanning trees of G .

Red edges can be deleted from G without impacting the final set of efficient spanning trees. In case $e = [u, v]$ is determined to be a blue edge, u and v can be contracted to build a new node w with $\delta(w) = (\delta(u) \cup \delta(v)) \setminus \{u, v\}$. Once w is built, u and v can be deleted from G .

Interestingly, the conditions for an edge to be blue or red can be checked in polynomial time by running two Depth First Searches for every edge in E . Thus, as noted in Sourd and Spanjaard [2008], the preprocessing runs in $\mathcal{O}(m^2)$. From now on, we only consider input graphs to our MO-MST instances that do not contain blue or red edges. By doing so, we assume that the described preprocessing phase is conducted before starting any actual MO-MST algorithm.

2.3 Pruning parallel transition arcs

The red and the blue criteria for edges in E , reduce the size of the input graph G . In other words, a red or a blue edge in G has no arc copies (cf. Definition 7) in \mathcal{G} . Using the condition that we derive in this section, we

are only able to delete a subset of an edge's arc copies. In this sense, the condition from Lemma 13 is more *local* than the blue/red edge conditions.

The condition is motivated by an almost trivial condition that holds for every One-to-One MOSP instance.

Lemma 12. *Let $(\mathcal{G}, \gamma, \{s\}, V)$ be a One-to-One MOSP instance. If \mathcal{G} contains two parallel arcs a, a' s.t. $\gamma(a) \leq \gamma(a')$ and $\gamma(a) \neq \gamma(a')$ then a' is not contained in any efficient $\{s\}$ - V -path.*

The condition becomes more powerful if we study the condition's meaning regarding the preimage edges of the involved arcs.

Lemma 13. *Let U be a node set in G containing s and $[u, w], [u', w]$ edges in $\delta(U)$ with $u, u' \in U$ and $w \in V \setminus U$. If $[u, w]$ dominates $[u', w]$, $[u', w]$ is not contained in any efficient spanning tree of G that contains an efficient spanning tree of U as a subtree.*

Proof. Let t_U be an efficient spanning tree of U contained in an efficient spanning tree t of G . If t contains an edge $e = [u, w] \in \delta(U)$ with $u \in U$ and $w \notin U$ e must not be dominated by any edge $e' = [u', w] \in \delta(U)$ because otherwise $t \circ e$ would be dominated by $t \circ e'$. Thus, $t \circ e$ would not be an efficient spanning tree of $U \cup \{w\}$ which contradicts Theorem 5. \square

To explain the latter condition in terms of the transition graph, consider a transition node $U \in \mathcal{V}$. We call every transition node $W \in \mathcal{V}$ a *successor node of U* if there exists a path from U to W in \mathcal{G} . Since \mathcal{G} is acyclic (cf. Remark 1), this notion is well defined. Assume there exists a dominance relation between parallel outgoing arcs of U , i.e., between two arcs $a, a' \in \delta^+(U)$ whose head node is a transition node $W = U \cup \{w\}$ for some $w \in G$. Then, if a' is dominated by a , no copies of the preimage edge a'^{-1} need to be considered when building the sets $\delta^+(W')$ for any transition node W' that is a successor node of U .

2.4 Pruning dominated outgoing arcs

Our last condition to remove arcs from the transition graph is the most local one: if an arc $a \in \mathcal{A}$ fulfills the condition in Lemma 14, we cannot gain further information concerning other arc copies from the preimage edge a^{-1} . Instead, the new condition only allows us to remove the arc a .

Lemma 14. *Consider a MO-MST instance $(G = (V, E), c)$ and assume w.l.o.g. that every spanning tree of G is rooted at a fixed node $s \in V$. Let t*

be an efficient spanning tree. For every edge $e \in t$ there is a cut $\delta(U)$ in G and a minimum complete set $\delta(U)^*$ of efficient cut edges s.t. $e \in \delta(U)^*$.

Proof. Fix an edge e from t and consider the two disjoint trees t_U and t_W obtained after removing e from t . We assume that t_U is the one containing the root node s and set $U = V(t_U)$ to be its node set. Clearly, e is a cut edge in $\delta(U)$ and any other cut edge e' connects t_U and t_W hence building a new spanning tree t' of G . If we suppose that a cut edge e' in $\delta(U)$ dominates e we get

$$c(t) = c(t_U) + c(e) + c(t_W) \leq c(t_U) + c(e') + c(t_W) = c(t').$$

and for at least one index $i \in \{1, \dots, d\}$, $c_i(t) < c_i(t')$ implying t' 's dominance and thus contradicting the statement's assumption. \square

A consequence of the last lemma is that when building the transition graph $\mathcal{G} = (\mathcal{V}, \mathcal{A})$ we do not need to include arc copies in $\delta^+(U)$ of edges that are dominated in the cut $\delta(U)$ of G . Assume the edge $e \in \delta(U)$ is dominated but contained in an efficient spanning tree t of G . Lemma 14 guarantees that there is a node set $W \subset V$ for which e is an efficient cut edge in $\delta(W)$. Then, e is contained in a set of outgoing arcs $\delta^+(W)^*$ of the transition node $W \in \mathcal{V}$. All in all, we obtain the following result.

Theorem 15. *Consider a MO-MST instance $(G = (V, E), c, s)$ without blue or red arcs in G . Any minimum complete set of efficient $\{s\}$ - V -paths in the Pruned Transition Graph $\mathcal{G}^* = (\mathcal{V}, \mathcal{A}^*)$ with $\mathcal{A}^* := \cup_{U \in \mathcal{V}} \delta^+(U)^*$ corresponds to a minimum complete set of efficient $\{s\}$ - V -paths in \mathcal{G} .*

Remark 2 (Incoming Arcs). From now on, we refer to the sets of incoming arcs of a transition node $W \in \mathcal{V}$ by $\delta^-(W)^*$ but the notation can be misleading. We use it to emphasize that we only consider a transition graph with the set \mathcal{A}^* of arcs. However, even if the sets $\delta^+(U)^*$ do not contain dominated arcs for any $U \in \mathcal{V}$, the set $\delta^-(W)^* := \{(U, W) \mid (U, W) \in \mathcal{A}^*\}$ can contain arcs that dominate each other.

Note that Lemma 14 is inspired by a pruning condition introduced in Chen et al. [2007, Section 3.2.]. In fact, the pruned spanning subtrees therein and in our Lemma 14 are the same. However, the authors in Chen et al. [2007] formulate the condition as a tree-dependent condition. For us it is important to formulate Lemma 14 as a cut-dependent condition s.t. it needs only to be checked once for every transition node U , when building $\delta^+(U)^*$.

3 New Dynamic Programming Algorithm

In the last section, we described the translation from a given MO-MST instance (G, c, s) with all trees rooted at a node $s \in V$ to the corresponding equivalent One-to-One MOSP instance $\mathcal{I}_{\text{SP}} = (\mathcal{G}^*, \gamma, \{s\}, V)$. In this section, we explain how to use a slightly modified version of the *Targeted Multiobjective Dijkstra Algorithm* (T-MDA) first published in [Maristany de las Casas et al., 2021a] for One-to-One MOSP instances like \mathcal{I}_{SP} . The peculiarity of such instances is that in practice, the transition graphs actually needed to solve the instance are much smaller than the theoretical upper bounds derived in (3) and (5). We are thus interested in a version of the T-MDA that does not store the transition graph explicitly. Instead, our new *Implicit Graph Multiobjective Dijkstra Algorithm* (IG-MDA) creates the graph implicitly as needed during the algorithm's execution. We describe the algorithm using One-to-One MOSP nomenclature only. However, to emphasize the equivalence to the original MO-MST instances, we still use capital letters to denote the transition nodes in \mathcal{G} , γ for the arc cost function, and for $U \in \mathcal{V}$, $T_{G(U)}^*$ to denote the minimum complete set of $\{s\}$ - U -paths computed in \mathcal{G} .

Recall that we are interested in minimum complete sets of efficient paths (cf. Definition 6). Thus, the IG-MDA only adds a new $\{s\}$ - U -path p to $T_{G(U)}^*$ if p is not dominated by nor equivalent to any path therein. To achieve this algorithmically, we introduce the following \preceq_D -operator.

Definition 16. Let $X \subset \mathbb{R}_{\geq 0}^d$ be a discrete set of cost vectors and $x' \in \mathbb{R}_{\geq 0}^d$. Then, $X \preceq_D x'$ is true if and only if there is an $x \in X$ s.t. $x \leq x'$.

Thus, p is added to $T_{G(U)}^*$ only if $\gamma(T_{G(U)}^*) \not\preceq_D \gamma(p)$ is not true. The lexicographic relation \prec_{lex} on $\mathbb{R}_{\geq 0}^d$ is defined as follows: for two vectors $x, y \in \mathbb{R}_{\geq 0}^d$, we write $x \prec_{lex} y$ if $x_i < y_i$ for the first index $i \in \{1, \dots, d\}$ for which $x_i \neq y_i$. The relation \preceq_{lex} is defined analogously.

Algorithm 1 is the pseudocode of the IG-MDA. It is a label setting algorithm (cf. [Maristany de las Casas et al., 2021b]) for One-to-One Multiobjective Shortest Path problems. In our pseudocode, we assume the existence of a container T^* that holds the lists $T_{G(U)}^*$ for every $U \in \mathcal{V}$. We discuss the details in the remainder to the section.

Paths in the algorithm are partitioned into two disjoint classes.

Permanent paths For every node $U \in \mathcal{G}$, the set $T_{G(U)}^*$ stores efficient and non-equivalent $\{s\}$ - U -paths that might be relevant for the reconstruction of efficient $\{s\}$ - V -paths stored in the minimum complete set

Algorithm 1: Implicit Graph Multiobjective Dijkstra Algorithm (IG-MDA)

Input : d -dimensional One-to-One MOSP instance $\mathcal{I}_{\text{SP}} = (\mathcal{G}^*, \gamma, \{s\}, V)$.

Output: Minimal complete set $T_{\mathcal{G}(V)}^*$ of $\{s\}$ - V -paths in \mathcal{G} w.r.t. γ .

```

1 Prio. queue of paths  $Q \leftarrow \emptyset$ ; // Lex. non-decreasing order w.r.t.  $\gamma$ .
2 Transition graph  $\mathcal{G}$  initialized only containing the transition node  $\{s\}$ ;
3 Trivial  $\{s\}$ - $\{s\}$ -path  $p_{\text{init}} \leftarrow ()$ ;
4  $Q \leftarrow Q.\text{insert}(p_{\text{init}})$ ;
5 while  $Q \neq \emptyset$  do
6    $p \leftarrow Q.\text{extractMin}()$ ;
7    $U \leftarrow$  last transition node of path  $p$ ; // If  $p = p_{\text{init}}$ ,  $U \leftarrow \{s\}$ .
8   success  $\leftarrow$  False;
9   if  $U \neq V$  then  $(Q, \text{success}) \leftarrow \text{propagate}(p, Q, T^*, \mathcal{NQP}, \beta_t)$ ;
10  if  $U == V$  or success == True then  $T_{\mathcal{G}(U)}^*.\text{append}(p)$ ;
11  New queue path  $p'$  for  $U \leftarrow$  Solve (6) according to  $U$  and the existing
     $\mathcal{NQP}_a$  lists for  $a \in \delta^-(U)^*$ ;
12  if  $p' \neq \text{NULL}$  then  $Q.\text{insert}(p')$ ;
13 return  $P_V$ ;
```

$T_{\mathcal{G}(V)}^*$ of efficient $\{s\}$ - V -paths w.r.t. γ at the end of the algorithm. Thus, a path might become permanent during the algorithm and once it is label as such, it is stored until the end.

Explored paths Consider a transition node $U \in \mathcal{V}$ and an $\{s\}$ - U -path p in \mathcal{G} that the IG-MDA considers for the first time. p is an explored path if it is neither dominated by nor equivalent to a permanent path in $T_{\mathcal{G}(U)}^*$. In later iterations, the expansions of p along the outgoing arcs $(U, W) \in \delta^+(U)^*$ are considered. If at least one such expansion of p turns out to be an explored $\{s\}$ - W -path, p is made permanent and stored in $T_{\mathcal{G}(U)}^*$. Otherwise, p is discarded and never considered again. In any case, p is no longer an explored path after its expansions are considered. The IG-MDA stores explored paths in different datastructures.

Priority Queue A priority queue Q contains at most one explored $\{s\}$ - U -path for every $U \in \mathcal{V}$ at any point in time. The $\{s\}$ - U -path in Q , if there is any, is required to be a lex. smallest explored $\{s\}$ - U -path.

Next Queue Path (\mathcal{NQP}) Lists Other explored $\{s\}$ - U -paths, if there are any, are stored in so called \mathcal{NQP} lists. There is such a list

associated with every arc in \mathcal{A} . If the last arc of an explored $\{s\}$ - U -path p that is not stored in Q is the arc $a \in \mathcal{A}$, p is stored in the list \mathcal{NQP}_a . Every such list is also sorted in lex. non-decreasing order.

In every iteration of the IG-MDA, a lex. minimal explored path is extracted from the queue Q (Line 6). Assume p is an extracted $\{s\}$ - U -path for some node $U \in \mathcal{V}$. Since p is an explored path, it is not dominated by or equivalent to any path in $T_{G(U)}^*$ by definition. Since for any $U \in \mathcal{V}$ the explored path in Q is lex. minimal compared to other existing explored $\{s\}$ - U -paths, p is guaranteed to be an efficient $\{s\}$ - U -path in \mathcal{G} w.r.t. γ . Thus, when extracted from Q , the IG-MDA builds the expansions of p along the outgoing arcs in $\delta^+(U)^*$ to decide whether p is made permanent or can be discarded.

Algorithm 2: propagate.

Input : $\{s\}$ - U -path p , priority queue Q , permanent paths T^* , lists of explored paths \mathcal{NQP} .

Output: Updated priority queue Q and a boolean flag telling if the propagation of p was successful along at least arc in $\delta^+(U)^*$.

```

1 Flag success  $\leftarrow$  False;
2 if  $\delta^+(U)^*$  not initialized then build  $\delta^+(U)^*$  as described in Section 3.1 ;
3 for  $W \in \delta^+(U)^*$  do
4    $q \leftarrow p \circ (U, W)$ ;
5   if  $\gamma(T_{G(W)}^*) \preceq_D \gamma(q)$  then continue;
6   success  $\leftarrow$  True;
7   if  $Q$  does not contain an  $\{s\}$ - $W$ -path then
8      $Q.\text{insert}(q)$  ;
9   else
10     $q' \leftarrow \{s\}$ - $W$ -path in  $Q$ ;
11    if  $\gamma(q) \prec_{lex} \gamma(q')$  then
12       $Q.\text{decreaseKey}(W, q)$  ;
13      if not  $\gamma(q) \leq \gamma(q')$  then
14         $(U', W) \leftarrow$  last arc in path  $q'$ ;
15        Insert  $q'$  at the beginning of  $\mathcal{NQP}_{(U', W)}$ ;
16    else
17      if not  $\gamma(q') \leq \gamma(q)$  then Insert  $q$  at the end of  $\mathcal{NQP}_{(U, W)}$  ;
18 return  $(Q, \text{success})$ ;

```

The decision is made in the subroutine propagate called in Line 9 of the IG-MDA. Consider an arc $(U, W) \in \delta^+(U)^*$. If the new explored $\{s\}$ - W -path $q := p \circ (U, W)$ is neither dominated by nor equivalent to a path in

$T_{G(W)}^*$, q becomes an explored path and p is stored as a permanent path in $T_{G(U)}^*$. If no expansion of p along an outgoing arc in $\delta^+(U)^*$ becomes a new explored path, p cannot be expanded to become an efficient $\{s\}$ - V -path in \mathcal{G} and is thus not needed and neglected. For every successful expansion of p along an outgoing arc $a = (U, W) \in \delta^+(U)$, the new explored $\{s\}$ - W -path q is stored as a new explored path. If there is no $\{s\}$ - W -path in Q , q is inserted into Q (Line 8). Otherwise, we assume q' to be the $\{s\}$ - W -path in Q and distinguish two cases. If $\gamma(q') \prec_{lex} \gamma(q)$ and q is neither dominated nor cost equivalent to q' , q is stored at the beginning of the list \mathcal{NQP}_a of its last arc $a \in \mathcal{A}$ Line 17. If $\gamma(q) \prec_{lex} \gamma(q')$, q substitutes q' in Q and Q is resorted. q' might re-enter the priority queue later since it can still become a permanent $\{s\}$ - W -path. Thus, if q' is neither dominated by nor cost equivalent to q , it is stored in the list $\mathcal{NQP}_{a'}$ of its last arc $a' \in \mathcal{A}$ Line 15. Inserting at the front or at the back of the \mathcal{NQP} lists depending on the case is explained in [Maristany de las Casas et al., 2021a, Lemma 4]. In both cases, the lists remain sorted in lex. non-decreasing order.

Besides the propagation of p as described in the last paragraph, every iteration of the IG-MDA needs to search for a new explored $\{s\}$ - U -path to be stored in the priority queue Q . Recall that for every node U , there is at most one $\{s\}$ - U -path in Q at any point in time and that this path, if it exists, is lex. minimal among all explored $\{s\}$ - U -paths. Thus, after the extraction of p from Q , a new explored $\{s\}$ - U -path p' might be inserted into Q . The explored $\{s\}$ - U -paths are stored in the \mathcal{NQP}_a lists for $a \in \delta^-(U)^*$ and thus, p' solves the minimization problem

$$\arg \text{lex min } \left\{ \gamma(p) \mid p \in \mathcal{NQP}_a, a \in \delta^-(U)^*, \text{ and not } \gamma(T_{G(U)}^*) \preceq_D \gamma(p) \right\}. \quad (6)$$

The minimization and the addition of p' to Q in case such a new explored path is found happen in Line 11 and Line 12 of Algorithm 1.

Further details on how the original T-MDA proceeds, its correctness, and further speedup techniques in the implementation can be read in [Maristany de las Casas et al., 2021a]. We now explain how \mathcal{G} is build and handled in the IG-MDA.

3.1 Implicit Handling of the Transition Graph

In this section we explain how the transition graph \mathcal{G} is managed implicitly in the IG-MDA. The addition of a node U to the initially empty set \mathcal{V} of transition nodes always entails the initialization of the list $T_{G(U)}^*$ since we assume that the algorithm will store some permanent $\{s\}$ - U -paths. No arcs

are added during this node initialization. At the beginning of the algorithm, the IG-MDA only adds the node $\{s\}$ to \mathcal{G} (Line 2).

When an $\{s\}$ - U -path p is extracted from the priority queue, expansions of p along outgoing arcs of U are built in propagate. To this aim, the set $\delta^+(U)^*$ needs to be constructed if it does not yet exist (Line 2 of propagate). The construction happens using (2) and the arc removal techniques discussed in Lemma 13 and Lemma 14. The creation of an arc (U, W) in this set requires

- the addition of (U, W) to the set $\delta^+(U)^*$,
- the addition of W to \mathcal{V} as explained in the last paragraph, if it does not yet exist,
- the addition of (U, W) to $\delta^-(W)^*$,
- and the initialization of the list $\mathcal{NQP}_{(U,W)}$

In case the set $\delta^+(U)^*$ already exists when p is extracted from the queue, we are sure that the lists $\mathcal{NQP}_{(U,W)}$ that are possibly needed in propagate are already initialized and that the new explored paths $q = p \circ (U, W)$ obtained from p 's expansions can be made permanent, i.e., added to $T_{G(W)}^*$, if needed later.

3.2 Running Time

Using the running time bound for the T-MDA derived in [Maristany de las Casas et al., 2021b], the number of nodes (3), and the number of arcs (5) in \mathcal{G} , we obtain the following result.

Theorem 17. *Consider an MO-MST instance (G, c, s) and the corresponding One-to-One MOSP instance $\mathcal{I}_{SP} = (\mathcal{G}^*, \gamma, \{s\}, V)$. Using the IG-MDA to solve \mathcal{I}_{SP} , setting $N_{\max} := \max_{U \in \mathcal{V}} |T_{G(U)}^*|$, and applying Theorem 10, (G, c, s) can be solved in*

$$\mathcal{O} \left(dN_{\max} \left(|\mathcal{V}| \log |\mathcal{V}| + |\mathcal{A}| N_{\max} \right) \right).$$

4 Experiments

All codes, results, and evaluation scripts used to generate the contents in this section are publicly available in [Maristany de las Casas, 2023].

4.1 Implementation Details

As noted in the introduction, when choosing a benchmark algorithm for our experiments in Section 4, we benefit from the extensive survey on MO-MST algorithms by Fernandes et al. [2020]. For more than two objectives, our use case, the best results are obtained using the *Built Network* (BN) algorithm, a dynamic programming algorithm originally published in Santos et al. [2018]. We explain the details of our implementation of the BN algorithm and assess its efficiency in A.

The deletion of red and blue edges from the original input graphs as explained in Section 2.2 is done in a preprocessing stage and both algorithms work on the resulting graphs without red or blue edges. In [Fernandes et al., 2020, Table 13] the authors list the number of red and blue edges in many MO-MST instances that we use in our experiments. In our code, we do no further manipulation of the input data.

A technique used by Pulido et al. [2014] to speedup the \preceq_D dominance checks is called *dimensionality reduction*. We already used it in [Maristany de las Casas et al., 2021a] to design the T-MDA and obtained a considerable speedup. Dimensionality reduction is used in conjunction with lexicographic sorting of explored paths. This sorting implies $\gamma_1(p) \leq \gamma_1(p')$ if a path p' is extracted from the queue after a path p . Thus, to determine whether p' is dominated by p , it suffices to compare the remaining $(d - 1)$ cost dimensions. Further implications of this technique are discussed in detail in [Pulido et al., 2014, Maristany de las Casas et al., 2021a]. Note that in [Santos et al., 2018] the authors achieved their fastest running times using the *sum of cost components* as the sorting criteria for explored paths. Also in our experiments this criteria yields better running times than lex. sorting. However, adding the dimensionality reduction technique to the BN algorithm when using lex. sorting, the overall running time is clearly better than using the sum of cost components as sorting criteria. Therefore, we report the results obtained from our BN implementation using lex. sorting and the dimensionality reduction technique.

Further implementation details such as the representation of paths using labels and the usage of a memory pool to avoid memory fragmentation can be read in [Maristany de las Casas et al., 2021a] or in our source code [Maristany de las Casas, 2023] directly. The running time of our implementation of the BN algorithm is dominated by the computation of minimal paths (cf. Definition 18). Thus, it is worth noting that for every explored path, we store a vector that indicates the order in which nodes of G are added to the corresponding tree. We then use this vector in Line 11 of Algorithm 3 to be

able to recognize relevant outgoing arcs faster in every iteration.

Readers interested in further implementation details will notice that in [Maristany de las Casas et al., 2021a] the original T-MDA was designed for One-to-One MOSP problems in which a lower bound, also called heuristic, of the costs from any (transition) node to the target (transition) node is computed before the algorithm starts. However, since the transition graphs used in this paper for the MOSP calculations are implicit, we cannot derive good lower bounds in advance. Thus, while reading [Maristany de las Casas et al., 2021a] always assume that our lower bound on the efficient paths' costs is the zero vector.

4.2 Instance Description

SPACYC based instances from [Santos et al., 2018] The authors from [Santos et al., 2018] kindly gave us access to their instances from which we use the 3 and 4 MO-MST instances for our experiments. For each number of criteria, graphs with 5 to 14 nodes are generated. For each fixed number of n nodes, graphs with $m = ni$ edges for $i \in \{5, 10, 15, 20\}$ are generated. For each arc, the costs are generated randomly using the *SPACYC* generator from [Knowles and Corne, 2001]. Thereby, the cost criteria are not correlated and the costs are chosen from the interval $[0, 100]$.

Instances from [Fernandes et al., 2020] We also got access to the instances used in Fernandes et al. [2020]. In this paper, we use their 3 and 4 dimensional MO-MST instances. For each dimension, we consider grid graphs and complete graphs with varying number of nodes (see [Fernandes et al., 2020, Maristany de las Casas, 2023] for details). Additionally, instances were generated with anticorrelated and correlated edge costs. For a fixed problem dimension (3 or 4 cost criteria), a fixed number of nodes, and an edge costs type there are 30 different instances. Thus, for example, we consider 30 complete graphs with 12 nodes and anticorrelated edge costs functions with 3 cost criteria.

4.3 Computational Environment

All computations were run on a machine with an Intel Xeon Gold 6246 @ 3.30GHz processor. The source code, written in C++, was compiled using g++ v.7.5.0 using the compiler flag `-O3`. Both algorithms were granted 2h of time and 30GB of memory to solve each instance.

Indexing transition nodes depending on the node set from the original graph G that they represent is important in both algorithms. To achieve this, we use the `dynamic bitset` class from the `boost` library [Boost, 2022] and for every bitset of length $n-1$ (since the node s is fixed) we compute the corresponding decimal representation to obtain an index. By doing so, we restrict ourselves to graphs with at most 64 nodes in today’s 64bit systems. However, as we will see in this section, the amount of efficient trees in every considered graph type requires more than the available 30GB of memory before reaching our constraint on the number of nodes.

4.4 Results

In this section we finally report the results obtained from our comparison between the IG-MDA and the BN algorithm implemented in [Maristany de las Casas, 2023]. Note for small input graphs, the obtained running times were below 0.01s for both algorithms. In the tables in this section, we do not report results for any group of graphs for which both algorithms solved the instances in less than 0.01s. However, in the `results` folder in [Maristany de las Casas, 2023], all results can be accessed and we also included the scripts used to generate the full tables and plots from this section. Also, for every table in the upcoming subsections, we pick a scatter plot corresponding to the running times of both algorithms that lead to one representative line of the table. The remaining scatter plots, one per line, are also stored in the `results` folder in [Maristany de las Casas, 2023].

4.4.1 Results from SPACYC based instances

In Table 1 we summarize the results obtained from the SPACYC based instances. Both algorithms solve every instance. While in 3d the BN algorithm is faster than the IG-MDA on instances with less than 8 nodes, this effect disappears in 4d, where the IG-MDA outperforms the BN algorithm consistently for all graph sizes. In both dimensions, the speedup grows with the input graph size and reaches $\times 16.76$ on the 3d instances and $\times 15.04$ on the 4d instances. Thereby, the IG-MDA performs better regarding the metrics *iterations per second* and *iterations per efficient spanning tree*. The second metric also implies that the IG-MDA solves the instances in less iterations since the number of efficient spanning trees depends on the instances and not on the algorithm. Figure 2 and Figure 4 show, for graphs with 10 to 14 nodes, the number of iterations that the IG-MDA and the BN algorithm performed per second. The IG-MDA outperforms the BN algorithm

Table 1: SPACYC based 3d and 4d instances. For every considered node cardinality $|V|$, 20 instances were considered. Both algorithms solved every instance. Numbers are geometric means.

$ V $	$ T_G^* $	BN			IG MDA			Speedup
		$ \mathcal{V} $	Iterations	Time	$ \mathcal{V} $	Iterations	Time	
3d edge costs								
10	398.14	477.71	17846.60	0.0318	312.88	7496.75	0.0060	5.27
11	487.21	774.66	36049.40	0.0695	526.56	14310.60	0.0122	5.70
12	815.86	1609.97	107572.10	0.3579	1179.25	41966.32	0.0421	8.50
13	1073.61	3111.80	252588.01	1.3572	1789.97	76472.73	0.0882	15.39
14	1747.29	6835.16	862549.99	8.4189	4288.41	259474.39	0.5023	16.76
4d edge costs								
9	1146.20	241.41	15941.44	0.0461	197.35	10460.27	0.0163	2.83
10	3014.38	471.18	66369.32	0.5246	413.88	43938.54	0.1431	3.66
11	4532.14	996.44	195159.07	2.7925	859.96	120389.30	0.5378	5.19
12	9060.48	2002.31	705053.83	30.8805	1705.53	409772.59	3.7650	8.20
13	13471.15	3734.22	1859534.46	190.0873	3196.62	1061076.64	17.2987	10.99
14	20735.06	7470.75	5051489.41	862.0660	6237.86	2474854.74	57.3346	15.04

regarding this metric consistently. Particularly in Figure 4 we observe that both algorithms seem to converge. This is because the dominance checks (\preceq_D) become more complex as the number of efficient solutions in the sets $T_{G(U)}^*$ for transition nodes U increase. Since these sets are equal for both algorithms, both algorithms make the same effort to decide whether explored trees are dominated. If the iterations per second of both algorithms converge but the speedup in favor of the IG-MDA increases with the graph size, the IG-MDA must do less iterations than the BN algorithm. Indeed, this can be already observed in Table 1. In Figure 3 and Figure 5 we plot the iterations per efficient spanning tree needed by both algorithms. It becomes apparent regarding this metric, the effort made by the IG-MDA increases much slower as the graph size increases. Using *minimal paths* (cf. Definition 18), the BN algorithm needs to decide upon the relevance of new explored paths using dominance checks only. Using cost-dependent arc pruning techniques as described in Section 2.3 and Section 2.4, the IG-MDA avoids the expansion of every efficient $\{s\}$ - U -path in $T_{G(U)}^*$ along a pruned arc (U, W) without doing dominance checks for every such path. In particular, being able to prune all incoming arcs of a transition node W leads to less transition nodes being considered in the implicit graphs of the IG-MDA algorithm (cf. $|\mathcal{V}|$ columns in Table 1).

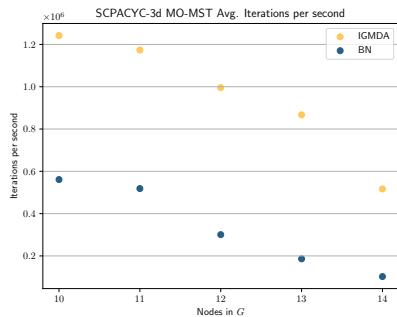


Figure 2: SPACYC 3d, avg. iterations/second

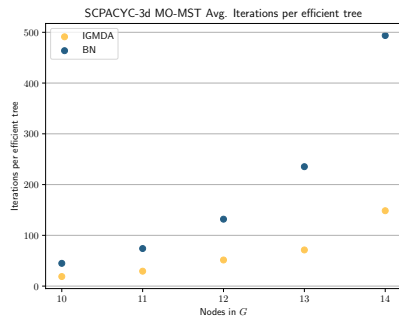


Figure 3: SPACYC 3d, avg. iterations/solution

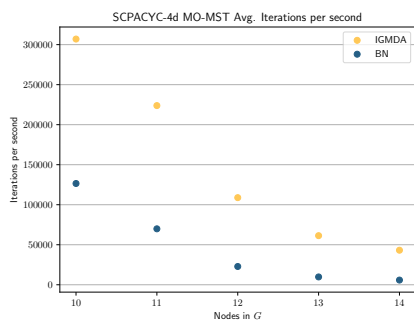


Figure 4: SPACYC 4d avg. iterations/second

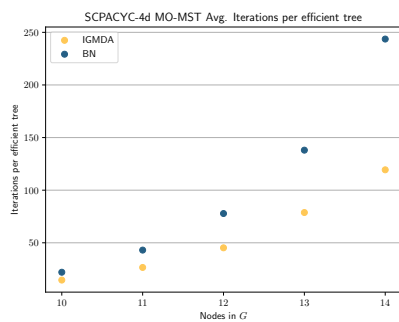


Figure 5: SPACYC 4d, avg. iterations/solution

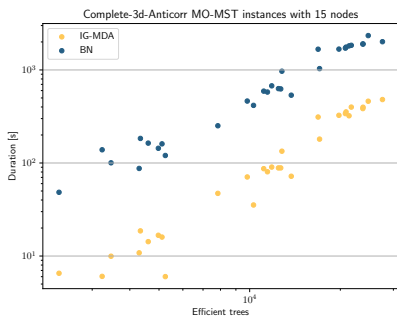


Figure 6: Complete-3d-Anticorr, 15 nodes

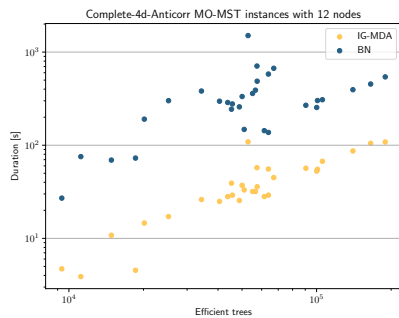


Figure 7: Complete-4d-Anticorr, 12 nodes

4.4.2 Results from Fernandes et al. instances

Table 2 and Table 3 summarize the results obtained from the instances from [Fernandes et al., 2020].

Complete Graphs with Anticorrelated Costs We report our results in Table 2. These instances are the most difficult ones. Both algorithms solve all instances with up to 12 nodes regardless of the edge cost dimension. Thereby, the IG-MDA is $\times 7.22$ faster on 3d instances and $\times 8.50$ faster on 4d instances. Additionally, the IG-MDA solves all 3d anticorrelated instances with 15 nodes and all but one with 17 nodes. Regarding the 4d instances, it solves 22 instances with 15 nodes. This is an improvement w.r.t. to the biggest instances of this type solved in [Fernandes et al., 2020] (12 nodes in 3d and 10 nodes in 4d). Note that the time limit is not the bottleneck. Instead, computations are aborted because of the memory limit of 30GB. Figure 6 and Figure 7 show the running times of both algorithms for some relevant graph sizes. The same plots for every other considered graph size are in the `result` folder from [Maristany de las Casas, 2023].

Grid Graphs with Anticorrelated Costs The results are summarized in Table 2. We observe the same trend as before regarding the speedups in favor of the IG-MDA. All instances with graphs with up to 18 nodes are solved in less than 0.01s by both algorithms. On 3d instances, both algorithms manage to solve all instances with up to 24 nodes. On bigger graphs, the BN algorithm solves a subset of the solved by the IG-MDA. The IG-MDA starts failing to solve instances on input graphs with 33 nodes. There are seven instances with 38 nodes that are solved by both algorithms (the IG-MDA solves 11/30 such instances) and on these instances the IG-MDA is $\times 68.16$ faster (cf. Figure 8). Note that the biggest instances from this group solved in [Fernandes et al., 2020] were grids with 20 nodes. The reason why the BN algorithm manages to solve some instances with 38 nodes even though it could not solve any instance with 36 nodes and only two with 33 nodes is that the seven solved instances with 38 nodes contain multiple blue and red edges. Thus, the actual input graphs for both algorithms are smaller (for details, see [Maristany de las Casas, 2023]). Regarding instances with 4d anticorrelated edge cost functions on grid graphs, both algorithms solve all instances with up to 24 nodes. The IG-MDA still solves all 30 instances with 27 nodes. From that size on the number of solved instances decreases because of the memory limit. The IG-MDA speedup on the instances with 24 nodes is $\times 2.99$ (see Figure 9). The relatively small number

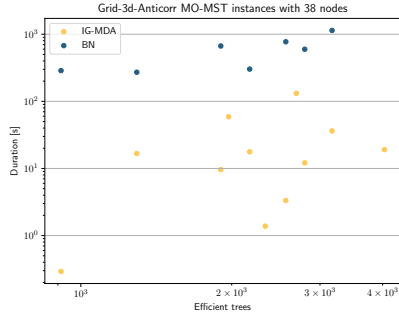


Figure 8: Grid-3d-Anticorr, 38 nodes

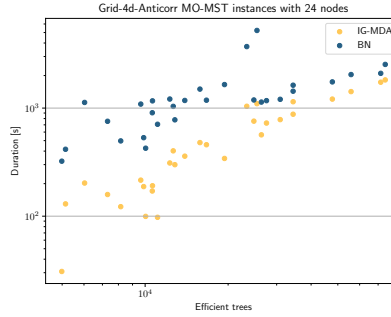


Figure 9: Grid-4d-Anticorr, 24 nodes

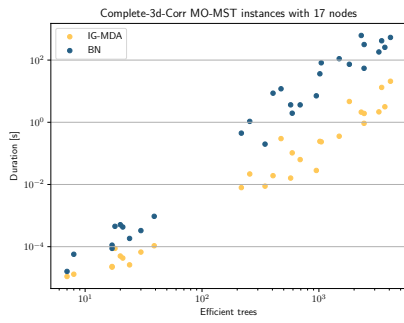


Figure 10: Complete-3d-Corr, 17 nodes

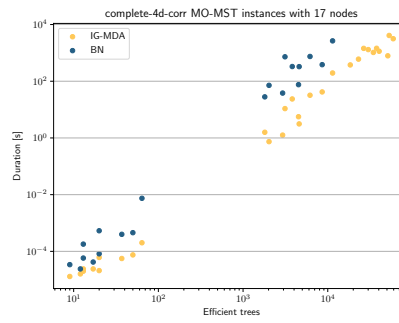


Figure 11: Complete-4d-Corr, 17 nodes

compared to other instance sets is because grids induce smaller transition graphs and, particularly on 4d instances, the running time is mostly determined by dominance checks (\preceq_D) that are equally time consuming for both algorithms.

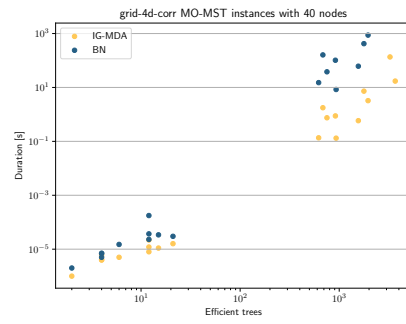
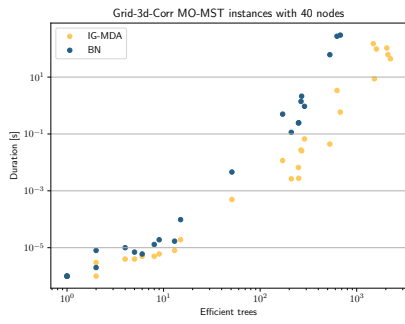


Figure 12: Grid-3d-Corr, 40 nodes Figure 13: Grid-4d-Corr, 40 nodes

Table 2: Instances from [Fernandes et al., 2020] with anticorrelated edge costs. Cardinality $|T_G|$ of solution sets, $|\mathcal{V}|$ of transition nodes, number of iterations, and time report geometric means built among solved instances only. The speedups consider only instances solved by both algorithms.

$ V $	Insts	BN					IG MDA					Speedup
		<i>Sol.</i>	$ T_G^* $	$ \mathcal{V} $	Iterations	Time	<i>Sol.</i>	$ T_G $	$ \mathcal{V} $	Iterations	Time	
COMPLETE 3d anticorr. edge costs												
10	30	30	1934.17	509.62	79059.14	0.4	30	1934.17	477.88	58042.67	0.08	4.82
12	30	30	4042.89	2039.89	668348.06	7.68	30	4042.89	1868.86	434829.76	1.27	6.03
15	30	30	10507.52	16344.5	13781596.11	530.79	30	10507.6	15166.2	8203636.87	73.52	7.22
17	30	10	8995.82	65151.83	39926366.12	4545.6	29	16773.63	60128.77	50138867.03	775.91	10.22
GRID 3d anticorr. edge costs												
18	30	30	327.46	1970.48	27559.31	0.0444	30	327.46	1059.14	15957.42	0.0105	4.24
20	30	30	507.80	4321.96	80646.78	0.1788	30	507.80	2081.46	41301.82	0.0354	5.05
24	30	30	1905.73	289945.96	12561838.13	119.8732	30	1905.73	108148.81	4556890.58	19.8963	6.02
27	30	25	2055.18	658592.00	32710242.90	331.8889	30	2432.92	243115.52	13189507.15	77.9690	7.27
30	30	8	1400.97	798812.92	32607409.69	336.6812	20	2119.93	238092.28	13277318.30	75.8248	31.61
33	30	2	2091.47	1353679.98	68100519.74	728.4824	16	3285.21	637610.27	44246349.41	341.4173	26.16
36	30	0	–	–	–	–	10	2945.52	497406.55	34694216.43	263.5790	–
38	30	7	1959.45	938641.43	51235269.92	504.1519	11	2189.33	35140.31	2977740.76	10.8611	68.16
40	30	0	–	–	–	–	2	3440.77	1310244.04	98125888.60	874.0739	–
COMPLETE 4d anticorr. edge costs												
10	30	30	14261.89	511.50	275211.78	3.61	30	14261.89	499.37	242326.48	0.85	4.27
12	30	30	49937.31	2046.63	3635468.74	266.18	30	49937.32	2006.20	2951674.07	31.32	8.50
15	30	0	–	–	–	–	22	200339.04	16224.95	77909983.48	4468.7791	–
GRID 4d anticorr. edge costs												
18	30	30	1605.54	3338.71	83063.06	0.1761	30	1605.54	2548.04	65344.60	0.0742	2.37
20	30	30	2022.36	6941.00	211043.31	0.5899	30	2022.36	4681.20	144836.59	0.2144	2.75
24	30	30	17036.10	487336.31	56591949.94	1145.0088	30	17036.10	308131.18	35528444.71	382.9531	2.99
27	30	12	10091.80	830056.49	70224110.93	1539.2769	30	21918.58	606263.90	83839892.33	1092.2398	5.93
30	30	0	–	–	–	–	8	21205.22	955448.68	133902354.68	2850.7280	–
33	30	0	–	–	–	–	2	13126.77	1776005.39	207538764.46	3671.7716	–

The results from the instances with correlated edge cost functions are reported in Table 3. As expected, the size of the solved instances is bigger than in the anticorrelated counterparts. However, this effect can be misleading. As we can observe in the scatter plots in Figure 10 to Figure 13 the running times of both algorithms are separated into two clusters. The reason is that with correlated costs, the preprocessing phase sometimes recognizes many blue and red arcs (cf. Section 2.2) s.t. the input graph for the MO-MST algorithms is actually very small. In fact, there are even 3d grid instances with 36 nodes that contain 35 blue arcs s.t. the remaining graph consists only of one node. The 35 blue arcs constitute the only efficient spanning tree for this instance. On grid graphs with a fixed number of nodes, the running times of both algorithm can differ by more than eight order of magnitudes (cf. Figure 13). Therefore, the geometric means in Table 3 are almost always clearly below one second but they need to be put into the context described in this paragraph. Only then, given the low average running times, we can understand that not all instances are solved.

Complete Graphs with Correlated Costs On 3d instances on complete graphs (Table 3), both algorithms solve all instances with up to 17 nodes where the IG-MDA is $\times 29.09$ faster (Figure 10). The IG-MDA also solves all instances with 22 nodes in 1.06s on average. In this group of instances, the BN algorithm solves 19/30 instances. Even though the edge costs are correlated, the instances on complete graphs with 4d edge costs are difficult and the BN algorithm cannot solve all instances with 15 nodes. On these graphs, the speedup in favor of the IG-MDA is $\times 15$; higher than on the same graphs with 3d edge costs.

Grid Graphs with Correlated Costs The lower left clusters in Figure 12 and Figure 13 show that indeed a considerable amount of instances in this group are almost solved during preprocessing. After deleting red edges and contracting blue ones, the remaining instances are so small that both MO-MST algorithms solve them in less than a millisecond. Overall, the IG-MDA remains consistently more than an order of magnitude faster than the BN algorithm on this type of instances (cf. Table 3). After deleting red edges and contracting blue edges, we are left with 12 instances with 4d edge costs and 30-31 nodes. To the best of our knowledge these instances are the biggest considered in the literature so far and the IG-MDA solves them in 329.9s on average (geo. mean). This data is extracted from the file `results/multiPrim_grid_corr_4d.csv` in [Maristany de las Casas, 2023].

Table 3: Instances from [Fernandes et al., 2020] with correlated edge costs. Cardinality $|T_G|$ of solution sets, $|\mathcal{V}|$ of transition nodes, number of iterations, and time report geometric means built among solved instances only. The speedups consider only instances solved by both algorithms.

$ V $	Insts	BN					IG MDA					Speedup
		<i>Sol.</i>	$ T_G^* $	$ \mathcal{V} $	Iterations	Time	<i>Sol.</i>	$ T_G $	$ \mathcal{V} $	Iterations	Time	
COMPLETE 3d corr. edge costs												
15	30	30	195.18	786.77	16508.49	0.0438	30	195.18	324.67	4988.89	0.0038	11.50
17	30	30	276.97	3240.53	101568.59	0.4329	30	276.97	769.99	14026.10	0.0149	29.09
20	30	22	289.40	6793.78	186354.27	0.7750	30	626.75	4364.52	109898.99	0.2118	35.26
22	30	19	228.20	6070.89	154896.66	0.5645	30	847.30	10209.11	390923.30	1.0635	24.93
GRID 3d corr. edge costs												
33	30	30	77.65	915.59	7991.91	0.0185	30	77.65	176.45	2042.85	0.0013	14.42
36	30	28	76.38	1521.15	15417.74	0.0808	30	93.14	342.61	4519.75	0.0037	18.52
38	30	30	56.21	396.92	3136.16	0.0060	30	56.21	89.00	966.31	0.0005	12.56
40	30	21	39.58	349.33	2406.14	0.3498	29	114.07	848.70	10929.89	0.0180	12.46
COMPLETE 4d corr. edge costs												
12	30	30	326.82	283.94	7713.31	0.0319	30	326.82	176.10	4076.06	0.0057	5.64
15	30	26	713.27	1646.49	81809.87	0.7962	30	1177.38	994.76	48608.53	0.1733	14.99
17	30	20	294.13	1191.90	31441.59	0.1965	30	1448.65	2110.19	124335.61	0.7096	11.50
20	30	13	305.19	2523.53	56573.88	0.1986	21	1444.82	3938.87	155447.82	0.6001	25.25
GRID 4d corr. edge costs												
24	30	30	89.11	690.09	5327.06	0.0135	30	89.11	221.65	2098.39	0.0020	6.79
27	30	30	167.53	1882.84	20551.53	0.0823	30	167.53	446.02	5610.28	0.0072	11.50
30	30	28	163.55	2795.94	35350.59	0.1349	30	216.40	840.08	13791.31	0.0216	13.05
33	30	23	82.51	669.94	5933.57	0.0141	29	206.47	842.73	14760.35	0.0222	9.27
36	30	20	49.51	311.78	2518.64	0.0057	27	193.85	812.96	13934.90	0.0225	11.20
38	30	26	144.41	806.94	11284.06	0.0347	30	235.57	352.92	8144.57	0.0112	11.46
40	30	18	66.30	598.21	4758.39	0.0153	20	98.46	234.39	3118.01	0.0036	12.27

5 Conclusion

The Implicit Graph Multiobjective Dijkstra Algorithm (IG-MDA) is a new dynamic programming algorithm for the Multiobjective Minimum Spanning Tree (MO-MST) problem. For its design we manipulated the transition graph defined in Santos et al. [2018] using cost dependent criteria to reduce its size and thus enhance the performance of the used algorithms. Dynamic programming for MO-MST problems entails solving an instance of the One-to-One Multiobjective Shortest Path problem arising transition graph. To solve this instance we use a modified version of the recently published Targeted Multiobjective Dijkstra Algorithm. In this paper, we analyzed the size of the transition graph to motivate its implicit handling in the IG-MDA. Storing the graph explicitly would otherwise lead to unreasonable memory consumption on many instances. To benchmark the performance of the IG-MDA, we compared it to our own version of the BN algorithm from [Santos et al., 2018] on a big set of instances from the literature. The results show that the IG-MDA is more efficient. To the best of our knowledge, it also manages to solve bigger instances than the biggest ones solved so far in the literature.

References

- S. Ahmadi, G. Tack, D. Harabor, and P. Kilby. Bi-Objective Search with Bi-Directional A*. In P. Mutzel, R. Pagh, and G. Herman, editors, *29th Annual European Symposium on Algorithms (ESA 2021)*, volume 204 of *Leibniz International Proceedings in Informatics (LIPIcs)*, pages 3:1–3:15, Dagstuhl, Germany, 2021. Schloss Dagstuhl – Leibniz-Zentrum für Informatik. ISBN 978-3-95977-204-4. doi: 10.4230/LIPIcs.ESA.2021.3.
- L. Amorosi and J. Puerto. Two-phase strategies for the bi-objective minimum spanning tree problem. *Int. T. Oper. Res.*, 29(6):3435–3463, 2022. doi: 10.1111/itor.13120.
- Boost. Boost C++ Libraries, Dec. 2022. URL <http://www.boost.org/>.
- A. Cayley. *A theorem on trees*, volume 13 of *Cambridge Library Collection - Mathematics*, pages 26–28. Cambridge University Press, 2009. doi: 10.1017/CBO9780511703799.010.
- G. Chen, S. Chen, W. Guo, and H. Chen. The multi-criteria minimum

spanning tree problem based genetic algorithm. *Inform. Sci.*, 177(22): 5050–5063, 2007. doi: 10.1016/j.ins.2007.06.005.

- L. Di Puglia Pugliese, F. Guerriero, and J. L. Santos. Dynamic programming for spanning tree problems: application to the multi-objective case. *Optim. Lett.*, 9(3):437–450, June 2014. doi: 10.1007/s11590-014-0759-1.
- M. Ehrgott. *Multicriteria Optimization*. Springer-Verlag, 2005. doi: 10.1007/3-540-27659-9.
- M. Ehrgott and X. Gandibleux. A survey and annotated bibliography of multiobjective combinatorial optimization. *OR Spectrum*, 22(4):425–460, Nov. 2000. doi: 10.1007/s002910000046.
- I. F. C. Fernandes, E. F. G. Goldberg, S. M. D. M. Maia, and M. C. Goldberg. Empirical study of exact algorithms for the multi-objective spanning tree. *Comput. Optim. Appl.*, 75(2):561–605, Mar. 2020. doi: 10.1007/s10589-019-00154-1.
- H. W. Hamacher and G. Ruhe. On spanning tree problems with multiple objectives. *Ann. Oper. Res.*, 52(4):209–230, Dec. 1994. doi: 10.1007/bf02032304.
- J. D. Knowles and D. W. Corne. A comparison of encodings and algorithms for multiobjective minimum spanning tree problems. In *Proceedings of the 2001 Congress on Evolutionary Computation (IEEE Cat. No.01TH8546)*, volume 1, pages 544–551, 2001. doi: 10.1109/CEC.2001.934439.
- J. B. Kruskal. On the shortest spanning subtree of a graph and the traveling salesman problem. *Proc. Amer. Math. Soc.*, 7(1):48–50, 1956.
- P. Maristany de las Casas. IG-MDA and BN Algo - Release for Preprint Citation, Apr. 2023. URL <https://doi.org/10.5281/zenodo.7842665>.
- P. Maristany de las Casas, L. Kraus, A. Sedeño-Noda, and R. Borndörfer. Targeted Multiobjective Dijkstra Algorithm. Dec. 2021a. Manuscript submitted for publication.
- P. Maristany de las Casas, A. Sedeño-Noda, and R. Borndörfer. An Improved Multiobjective Shortest Path Algorithm. *Comput. Oper. Res.*, 135:105424, 2021b. doi: 10.1016/j.cor.2021.105424.
- PassMark-Software. CPU Benchmarks, Apr. 2023. URL <https://www.cpubenchmark.net/compare/2448vs3521/>

Intel-i7-4720HQ-vs-Intel-Xeon-Gold-6246. Accessed April 27, 2023.

- R. C. Prim. Shortest connection networks and some generalizations. *Bell Syst. Tech. J.*, 36(6):1389–1401, 1957. doi: 10.1002/j.1538-7305.1957.tb01515.x.
- F. J. Pulido, L. Mandow, and J. L. Pérez de la Cruz. Multiobjective shortest path problems with lexicographic goal-based preferences. *Eur. J. Oper. Res.*, 239(1):89–101, Nov. 2014. doi: 10.1016/j.ejor.2014.05.008.
- R. M. Ramos, S. Alonso, J. Sicilia, and C. González. The problem of the optimal biobjective spanning tree. *Eur. J. Oper. Res.*, 111(3):617–628, 1998. doi: 10.1016/S0377-2217(97)00391-3.
- J. L. Santos, L. Di Puglia Pugliese, and F. Guerriero. A new approach for the multiobjective minimum spanning tree. *Comput. Oper. Res.*, 98: 69–83, 2018. doi: 10.1016/j.cor.2018.05.007.
- A. Sedeño-Noda and M. Colebrook. A biobjective Dijkstra algorithm. *Eur. J. Oper. Res.*, 276(1):106–118, July 2019. doi: 10.1016/j.ejor.2019.01.007.
- F. Sourd and O. Spanjaard. A Multiobjective Branch-and-Bound Framework: Application to the Biobjective Spanning Tree Problem. *INFORMS Journal on Computing*, 20(3):472–484, Aug. 2008. doi: 10.1287/ijoc.1070.0260.
- S. Steiner and T. Radzik. Computing all efficient solutions of the biobjective minimum spanning tree problem. *Comput. Oper. Res.*, 35(1):198–211, 2008. doi: 10.1016/j.cor.2006.02.023. Part Special Issue: Applications of OR in Finance.

A Build Network Algorithm

In this section, we briefly describe the *Build Network* (BN) algorithm from [Santos et al., 2018], using our terminology to easier compare it with the IG-MDA in what follows.

Again, we start with a given a MO-MST instance (G, c, s) and build the One-to-One MOSP instance $\mathcal{I}_{\text{SP}} = (\mathcal{G}, \gamma, \{s\}, V)$. Note that the original transition graph \mathcal{G} is used instead of \mathcal{G}^* . Then, the BN algorithm looks for efficient $\{s\}$ - V -paths w.r.t. γ in \mathcal{G} . Thereby, for every new explored path p the algorithm analyzes the ordering in which arcs were added to p to determine the allowed expansions of p . The conditions ensure that for every spanning tree of G the BN algorithm only considers one $\{s\}$ - V -path in \mathcal{G} that represents it. This is remarkable given that a tree with k nodes can have up to $(k - 1)!$ representations in \mathcal{G} as noted in Section 2.1. These unique representations of trees in \mathcal{G} are called *minimal paths*.

Definition 18 (Minimal Paths (cf. Definition 3.5. Santos et al. [2018])). Let $q = (a_1, \dots, a_k)$ be a path in \mathcal{G} with k arcs for some $k \leq n - 1$. For the arcs a_i , we set $a_i^{-1} = [u_i, w_i] \in E$. q is said to be a *minimal path* if it satisfies one of the following conditions:

1. $k = 1$
2. $k \geq 2$, the subpath $p = (a_1, \dots, a_{k-1})$ is a minimal path and there holds $u_{k-1} = u_k$, $w_{k-1} < w_k$.
3. $k \geq 2$, the subpath $p = (a_1, \dots, a_{k-1})$ is a minimal path and there exist to indices $\ell, \ell' \leq k$ with $\ell < \ell'$ and there holds $u_{k-1} = w_\ell$ and $u_k = w_{\ell'}$.

To understand the latter definition we consider the preimage edges $[u_i, w_i]$ of q as ordered pairs. Then, for the leading subpath p of q with i arcs, $i < k$, the node w_i is the $(i + 1)^{\text{th}}$ node added to the tree in G represented by q . Then, the last condition in Definition 18 states, in terms of paths in \mathcal{G} , that if w_ℓ is added to a spanning tree after $w_{\ell'}$, the adjacent nodes of w_ℓ must be considered prior to the adjacent nodes of $w_{\ell'}$. Additionally, the second condition, states that for a node u , its adjacent nodes have to be considered in order w.r.t. the considered indexing of the nodes in G . Then, the statement in Santos et al. [2018, Proposition 3.7.] is easy to see: there is a one-to-one correspondence between minimal paths in \mathcal{G} and trees in G .

The pseudocode of our implementation of the BN algorithm is in Algorithm 3.

Algorithm 3: Built Network (BN) algorithm.

Input : d -dimensional One-to-One MOSP instance $\mathcal{I}_{\text{SP}} = (\mathcal{G}^*, \gamma, \{s\}, V)$.

Output: Minimal complete set $T_{\mathcal{G}(V)}^*$ of efficient $\{s\}$ - V -paths in \mathcal{G} w.r.t. γ .

```

1 Priority queue of paths  $Q \leftarrow \emptyset$ ; // Sorted according to  $\gamma$ .
2 Transition graph  $\mathcal{G}$  initialized only containing the transition node  $\{s\}$ ;
3 Trivial  $\{s\}$ - $\{s\}$ -path  $p_{\text{init}} \leftarrow ()$ ;
4  $Q \leftarrow Q.\text{insert}(p_{\text{init}})$ ;
5 while  $Q \neq \emptyset$  do
6    $p \leftarrow Q.\text{extractMin}()$ ;
7    $U \leftarrow$  last transition node of path  $p$ ; // If  $p = p_{\text{init}}$ ,  $U \leftarrow \{s\}$ .
8   if  $\gamma(T_{\mathcal{G}(U)}^*) \preceq_D \gamma(p)$  then continue;
9   Boolean flag success  $\leftarrow$  False;
10  if  $\delta^+(U)$  not initialized then build  $\delta^+(U)$  as described in
    Appendix A.1 ;
11   $\mathcal{MIN}_p \leftarrow$  Minimal paths  $p \circ a$  for  $a \in \delta^+(U)$  ;
12  for  $q \in \mathcal{MIN}(p)$  do
13    Assume  $q$  is spanning tree of  $W \subseteq V$ ;
14    if not  $\gamma(\mathcal{P}_W) \preceq_D \gamma(q)$  then
15       $Q.\text{insert}(q)$ ;
16      success  $\leftarrow$  True;
17  if success == True then  $\mathcal{P}_U.\text{append}(p)$ ;
18 return  $\mathcal{P}_V$ ;

```

We combine the minimal path definition from [Santos et al., 2018] with a *lazy queue management approach* for explored paths that notably enhances the running time of label setting MOSP algorithms as experienced in [Ahmadi et al., 2021, Maristany de las Casas et al., 2021a]. Lazy queue management of explored paths works as follows. Assume the minimal $\{s\}$ - W -path q in \mathcal{G} is considered by the algorithm. It is immediately discarded (Line 14) if it is dominated by or equivalent to any path in $T_{G(W)}^*$. Otherwise, it is inserted into the algorithm’s priority queue Q without further checks (Line 15). This motivates the *lazy* attribute of this method since q is not compared to other explored $\{s\}$ - W -paths. Instead, because of the lex. ordering of paths in Q , q is extracted from Q after every explored $\{s\}$ - W -path q' with $\gamma(q') \preceq_{lex} \gamma(q)$. Note that this also holds for $\{s\}$ - W -paths that are added later than q but before q ’s extraction. These q' paths are the only explored $\{s\}$ - W -paths that can dominate q and they are possibly added to $T_{G(W)}^*$ before q is extracted. Thus, our version of the BN algorithm with lazy queue management repeats the dominance or equivalence check $\gamma(T_{G(W)}^*) \preceq_D \gamma(q)$ after q ’s extraction from Q (Line 8). Only if q turns out not to be dominated by or equivalent to any path in $T_{G(W)}^*$ after this check, it is further considered by the algorithm. In this case, the BN algorithm needs to evaluate the outgoing arcs in $\delta^+(W)$ s.t. only minimal paths arising from q ’s expansions are considered (Line 11).

The correctness of our implementation of the BN algorithm follows from the fact that considering minimal paths in \mathcal{G} suffices to find a minimum complete set of efficient paths that represent a minimum complete set of efficient spanning trees in G [Santos et al., 2018, Proposition 3.7.] and from the correctness of the NAMOA*-lazy algorithm introduced in [Maristany de las Casas et al., 2021a]. All in all, we have designed a new algorithm combining the elegant pruning rule (minimal paths) that made the original BN algorithm state of the art with recent advances used to improve the handling of explored paths in label setting MOSP algorithms.

A.1 Implicit Handling of the Transition Graph

Handling the transition graph \mathcal{G} implicitly is easier for the BN algorithm than for the IG-MDA. It works as described in Section 3.1 with the following two differences. First, neither lists of incoming arcs nor \mathcal{NQP} lists have to be maintained. Second, the lists of $\delta^+(U)$ of outgoing arcs for a transition node U are built in Line 10 as described in (2) without any arc removal conditions. For every $\{s\}$ - U -path p extracted from Q the relevant outgoing arcs needed to build minimal path expansions of p are chosen in a path-dependent way in Line 11. We suppose that the authors of Santos et al.

[2018] also generate the transition graph \mathcal{G} implicitly as described in this section to restrict the memory consumption of \mathcal{G} as far as possible.

A.2 Comparison to the IG MDA

There are two main differences between the IG-MDA and our new BN algorithm:

Explored paths The IG-MDA algorithm restricts the size of the queue and stores other explored paths in \mathcal{NQP} lists. It requires to search for a new queue path in every iteration but does not require a dominance or equivalence check after a path’s extraction from the queue. Our new BN algorithm stores multiple explored paths per node in the queue but requires dominance or equivalence checks right after every path’s extraction from the queue.

Pruning conditions The IG-MDA uses cost dependent criteria (Lemma 13, Lemma 14) to reduce the number of arcs in the transition graph in a path-independent way. The BN algorithm in its original version as well as in our implementation uses path-dependent pruning techniques (minimal paths, cf. Definition 18) forcing the inclusion of nodes in the represented spanning trees to follow a fixed order/rule.

Example 19 (Different Pruning Criteria). The path $p = ((1, 2), (1, 3), (1, 4))$ is minimal according to Definition 18 and represents the same tree than the path $p' = ((1, 2), (1, 4), (1, 3))$. The BN algorithm would discard the expansion of the subpath $((1, 2), (1, 4))$ along the arc $(1, 3)$ because it violates Item 2 in Definition 18. The IG-MDA allows this expansion of the path if the arc $(1, 3)$ is not dominated by any arc in the cut defined by the node set $\{1, 2, 4\}$. Note however that at the transition node $W = \{1, 2, 3, 4\}$ p and p' meet with equivalent costs and the \preceq_D operator guarantees that only one is kept and further expanded.

A.3 Efficiency of our BN implementation

We tried to determine whether our implementation of the BN algorithm from [Santos et al., 2018] is efficient. Since we do not have access to the original implementation from the authors, we extrapolated their computational results to the performance on our machine. Using [PassMark-Software, 2023] we found out that on single-threaded jobs the processor used in [Santos et al., 2018] delivers 76.3% of the performance of our processor. Thus we

Table 4: Comparison of BN algorithm implementations in [Santos et al., 2018] and in [Maristany de las Casas, 2023]. Computations using 3 and 4 dimensional SPACYC based instances.

Nodes	10	11	12	13	14
BN 3d in [Santos et al., 2018]	0.25	1.00	5.42	22.11	86.33
CPU scaled	0.19	0.76	4.14	16.87	65.87
BN 3d as in Algorithm 3	0.04	0.10	0.54	2.19	11.25
BN 4d in [Santos et al., 2018]	5.58	28.40	188.14	712.96	3656.91
CPU scaled	4.26	21.67	143.55	543.99	2790.22
BN 4d as in Algorithm 3	0.76	6.34	69.76	351.73	1737.88

scaled the average running times for the SPACYC based instances in Table 6 of [Santos et al., 2018] accordingly to obtain the expected running times of their code on our machine. In Table 4 we list the original running times from [Santos et al., 2018], the CPU-scaled running times we obtained, and the running times we obtained from our implementation of Algorithm 3. Since the BN implementation in [Santos et al., 2018] is coded in Java and ours is coded in C++, the running times are still not completely comparable. However, our running times seem to be good enough ($\times 6$ faster on the biggest 3d instances and $\times 1.6$ faster on the biggest 4d instances) to claim that our implementation of the BN algorithm is efficient and useful for the comparisons that follow in this paper. The speedup decreases notably with increasing edge cost dimension because the impact of dominance checks on running time increases in higher dimensions. Most probably, both programming languages are similarly efficient in performing these checks. Note that the reported running time averages in Table 4 do not coincide with those reported in Table 1. The reason is that in [Santos et al., 2018] the authors always use arithmetic means and in this paper we use geometric means everywhere except in Table 4.